

Aerosol first indirect effects on non-precipitating low-level liquid cloud properties as simulated by CAM5 at ARM sites

Chuanfeng Zhao,¹ Stephen A. Klein,¹ Shaocheng Xie,¹ Xiaohong Liu,² James S. Boyle,¹ and Yuying Zhang¹

Received 6 February 2012; revised 20 March 2012; accepted 26 March 2012; published 28 April 2012.

[1] We quantitatively examine the aerosol first indirect effects (FIE) for non-precipitating low-level single-layer liquid phase clouds simulated by the Community Atmospheric Model version 5 (CAM5) running in the weather forecast mode at three DOE Atmospheric Radiation Measurement (ARM) sites. The FIE is quantified in terms of a relative change in cloud droplet effective radius for a relative change in accumulation mode aerosol number concentration under conditions of fixed liquid water content (LWC). CAM5 simulates aerosol-cloud interactions reasonably well for this specific cloud type, and the simulated FIE is consistent with the long-term observations at the examined locations. The FIE in CAM5 generally decreases with LWC at coastal ARM sites, and is larger by using cloud condensation nuclei rather than accumulation mode aerosol number concentration as the choice of aerosol amount. However, it has no significant variations with location and has no systematic strong seasonal variations at examined ARM sites. **Citation:** Zhao, C., S. A. Klein, S. Xie, X. Liu, J. S. Boyle, and Y. Zhang (2012), Aerosol first indirect effects on non-precipitating low-level liquid cloud properties as simulated by CAM5 at ARM sites, *Geophys. Res. Lett.*, 39, L08806, doi:10.1029/2012GL051213.

1. Introduction

[2] Aerosols modify the Earth's radiation budget through direct effects and indirect effects on clouds. Among various aerosol indirect effects like cloud albedo effects, cloud amount effects, and cloud lifetime effects [Twomey, 1977; Albrecht, 1989; Ackerman et al., 2000], the influence of aerosols on the cloud droplet effective radius (r_e) with no change of cloud liquid water content (LWC) is called the aerosol first indirect effect (FIE). McComiskey and Feingold [2008] have shown that the radiative forcing of the aerosol indirect effects, which is the difference in radiative flux that occurs as a result of changes in cloud properties for post-versus pre-industrial aerosol concentrations, ranges from -3 to -10 W m⁻² for each 0.05 increment in FIE ($FIE = -\frac{\partial \ln r_e}{\partial \ln \alpha}$, where α is aerosol amount) for a mid-latitude and total cloud cover condition. Therefore, accurate quantification of FIE is significant for better prediction of climate change.

[3] Observational studies have shown various but mostly positive FIE for liquid clouds. Here positive FIE means that aerosol increases are accompanied by decreased cloud

droplet r_e and increased cloud droplet number concentration (N_d). By summarizing numerous observational studies utilizing ground-based, aircraft and satellite measurements [Han et al., 1994; Feingold et al., 2003; Kim et al., 2003; Garrett et al., 2004; Pandithurai et al., 2009; Costantino and Bréon, 2010], Shao and Liu [2006] and McComiskey and Feingold [2008] have shown the FIE generally lies between 0.02 and 0.33, with most values between 0.05 and 0.25. At the Atmospheric Radiation Measurement (ARM) program sites, Feingold et al. [2003] and Kim et al. [2008] have found FIE values of 0.02–0.17 for the Southern Great Plains (SGP) site and Garrett et al. [2004] have found FIE values between 0.11 and 0.19 for the North Slope of Alaska (NSA) site using its ground-based remote sensing instruments.

[4] The large variation of FIE seen in observations could be caused by multiple factors. As indicated by Tang et al. [2011], uncertainties in the correlation between aerosol loading and cloud properties may result from variability in geographical and seasonal conditions and other factors such as the vertical profiles of clouds and aerosols, aerosol physical and chemical properties, cloud geometric thickness, vertical wind shear, and horizontal wind convergence at cloud level. Some recent studies [Grandey and Stier, 2010; McComiskey and Feingold, 2012] show that substantial differences in FIE can also occur from averaging over a wide range of spatial resolutions. Furthermore, differences in the FIE among various studies might be also partly related to the use of different analysis methods [Rosenfeld and Feingold, 2003].

[5] The findings from observations provide an opportunity to evaluate aerosol-cloud interactions in climate models. This study will examine the FIE simulated in CAM5 [Neale et al., 2010], which is the 5th version of the National Center for Atmospheric Research (NCAR)/Department of Energy (DOE) Community Atmospheric Model. We will examine the simulated FIE at three ARM sites, NSA, SGP and Tropical West Pacific at Darwin (TWP) in order to span a wide range of latitudes and sample both near-ocean and land conditions. The simulated FIE will be compared to observational studies of FIE that used data collected at these sites. Note that we focus on non-precipitating low-level liquid clouds both to avoid complications of precipitation and ice-microphysics, because the observational constraints are more robustly determined for this cloud type relative to other cloud types.

2. Method for FIE Calculation

[6] The aerosol FIE is generally quantified by $FIE = -\frac{\partial \ln r_e}{\partial \ln \alpha}$ or $FIE = \frac{1}{3} \frac{\partial \ln N_d}{\partial \ln \alpha}$, where α represents aerosol number concentration, aerosol optical depth, or other aerosol related variables. The factor of 1/3 appears because $r_e \propto N_d^{-1/3}$ for a

¹Atmosphere, Earth, and Energy Division, Lawrence Livermore National Laboratory, Livermore, California, USA.

²Pacific Northwest National Laboratory, Richland, Washington, USA.

constant LWC. However, observational studies show the FIE determined using cloud r_c and that determined using N_d can be different from each other due to the different degrees of inhomogeneous mixing with ambient drier air between clean and polluted clouds [Shao and Liu, 2006]. For CAM5 simulations, they are really identical because of the functional fit assumed in the parameterization of the cloud droplet size distribution (i.e., there are only two degree of freedom between N_d , r_c , and LWC). Therefore, we will only report the FIE obtained using cloud droplet r_c for a given LWC,

$$FIE = - \left(\frac{\Delta \ln r_c}{\Delta \ln \alpha} \right)_{LWC}. \quad (1)$$

3. CAM5 Simulation

[7] CAM5 includes a modal aerosol module (MAM) [Liu et al., 2011] to predict aerosol mass and number concentrations. By combining the MAM and a two-moment cloud microphysics scheme [Morrison and Gettelman, 2008], one can study aerosol-cloud interactions for the first time in CAM.

[8] Model results in this study are from CAM5 hindcast integrations conducted by the DOE supported Cloud-Associated Parameterizations Testbed (CAPT) project [Phillips et al., 2004] for the period from June 2008 to May 2010. Different from CAM5 climate integrations, which represent the statistics of atmospheric states and are not initialized to any specific time, the CAPT approach integrates climate models in short-range forecast mode by initializing climate models with realistic atmospheric states from reanalysis data produced by numerical weather prediction centers. We expect the results shown here to apply to climate integrations of CAM5, although some quantitative differences are possible.

[9] A series of 5-day forecasts were generated with CAM5 by initializing the model every day at 0000 UTC from European Centre for Medium-Range Weather Forecasts analysis for the entire period. Hourly data from forecast hours 24 to 48 were concatenated into a continuous time series that was examined in this study. Using this time range effectively reduces the impact of model spin-up that may occur during the first few hours of an integration, but is close enough to the start of each forecast such that we can be sure that the atmospheric state is still close to the observation. If so, we assume that model errors can be primarily linked to deficiencies in model physics. Model results at the closest 4 grid points to the selected ARM sites are used in this study. Note that CAM5 has a horizontal resolution of about 1° and 30 vertical layers.

[10] In the following analysis, we locate the conditions for non-precipitating low-level single-layer liquid clouds by selecting levels and hours in which a low-level cloud (below 700 hPa) is present and with no middle or high clouds, the liquid and ice precipitation rate (P) is less than 0.086 mm/day at all vertical layers from the cloud to the surface, the horizontal area coverage of low clouds is above 50%, the clouds are single-layer and have only liquids, and the cloud N_d is greater than 1 cm^{-3} . Aerosol information used to quantify FIE is selected from the same levels and times which meet these conditions. Note that there are only a small fraction

(<5%) of single layer liquid clouds with N_d less than 1 cm^{-3} . Considering that there are almost no clouds with $P = 0$ at all vertical layers, $P < 0.086 \text{ mm/day}$ instead of $P = 0$ is used to define non-precipitating clouds. It shows that the results in the following analysis are not sensitive to the small P threshold value.

4. Evaluation of Simulated Aerosol and Cloud Properties

[11] Before presenting our analysis of the FIE, we evaluate the ability of CAM5 to simulate realistic aerosol and cloud properties. For statistical evaluation we use the ARM ground-based measurements of aerosol optical depths (AOD) from the Multi-Filter Rotating Shadowband Radiometer (MFRSR) [Harrison et al., 1994] for the same years and cloud properties from the ARM cloud retrieval ensemble dataset (ACRED) (C. Zhao et al., Toward understanding of differences in current cloud retrievals of ARM ground-based measurements, submitted to *Journal of Geophysical Research*, 2011) from 1997 through 2008. Because the MFRSR can only observe AOD during clear sky periods, we assume the performance of CAM5 in simulating AOD during clear sky periods can be applied to all periods.

[12] Figure 1 shows the intercomparisons of seasonally averaged non-precipitating low-level liquid cloud droplet r_c and clear sky AOD between ARM observation and CAM5 simulations with temporal standard deviation (outlines) at NSA, SGP and TWP. We note that the seasonal averages and temporal standard deviations of aerosol and cloud properties are based on hourly data from CAM5 simulations and ARM observations. In order to be comparable with the simulated clouds defined in section 3, we only consider non-precipitating single-layer liquid phase clouds with tops below 3 km from observations. 3 km is used to define the tops of low clouds from observations because it is roughly 700 hPa in height. Note that the averaged cloud droplet r_c shown in Figure 1 is in-cloud average within a season. Here, seasons are denoted by grouping months by their first initials (for instance, JJA is “June-July-August”).

[13] ACRED has two different cloud products for liquid cloud properties for each of examined ARM sites, which are denoted as obs1 and obs2 in Figure 1. Obs1 is the cloud product of MICROBASE and obs2 is SHUPE_TURNER at NSA, MACE at SGP, and COMBRET at TWP. The details about these cloud products are described by Zhao et al. (submitted manuscript, 2011). Both obs1 and obs2 are used in our study in order to take into account of potential cloud retrieval errors. Cloud droplet r_c simulated by CAM5 agrees reasonably well with the two observations at NSA. However, the simulated cloud droplet r_c is generally larger than both observational estimates and does not show as much variation across site and season as the observations at SGP and TWP. The weak seasonal variation of cloud droplet r_c in CAM5 may have an impact on the seasonal variation of simulated FIE due to the nature of regression calculation. While not shown in Figure 1, the LWC in simulated low-level liquid clouds mainly lie below 1 g m^{-3} with a large concentration of values around 0.1 g m^{-3} , consistent with those retrieved from ARM instruments (Zhao et al., submitted manuscript, 2011).

[14] The AOD simulated by CAM5 is generally comparable with ARM observations for clear sky periods except at

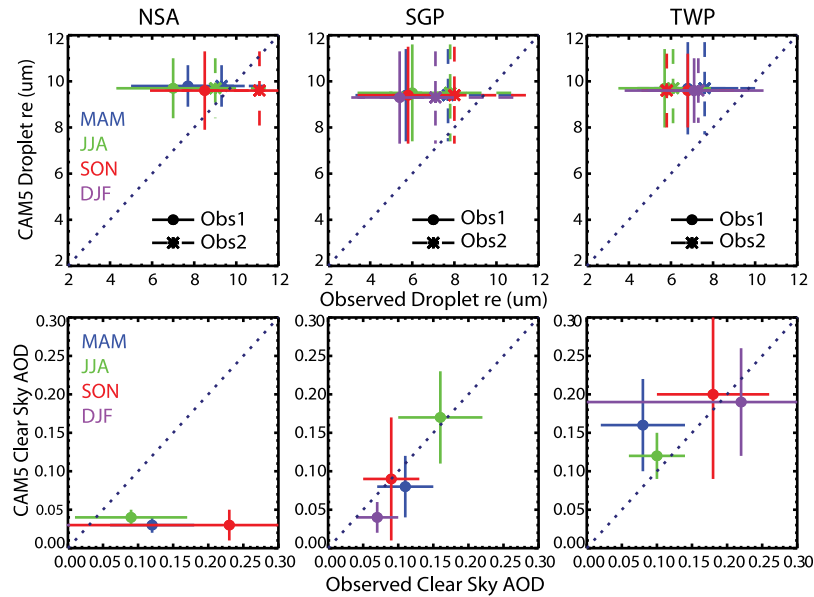


Figure 1. Intercomparison of seasonally averaged non-precipitating low-level liquid cloud droplet r_c and clear sky aerosol optical depth (AOD) between ARM observations and CAM5 simulations with temporal standard deviation (outlines) at NSA, SGP and TWP. Note that two different observations for cloud r_c have been used.

NSA where it is severely underestimated. Both CAM5 and observations show that the AOD has a maximum in summer (JJA at SGP and DJF at TWP) and a minimum in winter at SGP and TWP. At NSA, CAM5 simulations and ARM observations show opposite seasonal variations of AOD, indicating serious problems for the aerosol simulations at high latitudes in CAM5. The aerosol accumulation mode number concentration (N_a) and cloud condensation nuclei (CCN) number concentration (N_{CCN}) at 0.1% supersaturation ($S = 0.1\%$) simulated by CAM5 (Table 1) show a maximum in JJA and a minimum in DJF at both SGP and TWP. Observational studies have also shown that more accumulation mode aerosol and CCN ($S = 0.1\%$) are observed in JJA than other seasons due to stronger photochemical production of aerosols at SGP [Liu *et al.*, 2011], and due to more frequent continental winds rather than marine winds at TWP [Bouya and Box, 2011]. Therefore, CAM5 simulates the aerosol properties reasonably well at SGP and TWP.

5. The FIE in CAM5

[15] By screening the data in the way shown in Section 3, we eliminate the complications of other cloud types and conditions. However, we can still examine the sensitivity of FIE in selected clouds to factors such as geographical

location, season, LWC and choice of variable for aerosols. We begin our study examining FIE at the NSA site.

5.1. FIE at the NSA Site

[16] Figure 2 shows the relationship between aerosol accumulation mode N_a and cloud r_c for four ranges of LWC at NSA in spring, summer and fall of the period from June 2008 to May 2010. Winter is not shown because no low-level liquid clouds are found in that period. The solid lines in the plots are linear regression lines on a log scale. The FIE values with 95% confidence intervals to the linear least squares regression slope and the correlations between aerosol and cloud properties are shown in all figures. Only statistically significant FIE will be discussed in this study. Because the clouds with large LWC are often contaminated by precipitation, there are insufficient data samples for LWC greater than 0.4 g m^{-3} . Thus, we examine the FIE for LWC ranges of $0.01\text{--}0.05$, $0.05\text{--}0.1$, $0.1\text{--}0.2$ and $0.2\text{--}0.4 \text{ g m}^{-3}$.

[17] Figure 2 shows that the FIE has a range of $0.07\text{--}0.14$ and $0.09\text{--}0.18$ for summer and fall, respectively. Note that there are no statistically significant FIE in spring. Compared to the observational findings (FIE between 0.11 and 0.19) by Garrett *et al.* [2004] for liquid clouds between April and October at NSA, FIEs simulated by CAM5 are quite reasonable in summer and fall. However, Garrett *et al.* [2004]

Table 1. Seasonal Averages and Standard Deviations of Aerosol Accumulation Mode Number Concentration (N_a) and Cloud Condensation Nuclei (CCN) Number Concentration (N_{CCN}) at $S = 0.1\%$ Simulated by CAM5 During the Period Between June 2008 and May 2010^a

Site Season	$N_a \text{ (cm}^{-3}\text{)}$				$N_{CCN} \text{ (cm}^{-3}\text{)}$			
	MAM	JJA	SON	DJF	MAM	JJA	SON	DJF
NSA	103 ± 92	116 ± 136	153 ± 257	Nan	14 ± 17	14 ± 22	18 ± 29	Nan
SGP	244 ± 360	251 ± 289	212 ± 290	181 ± 264	82 ± 155	104 ± 162	84 ± 155	47 ± 84
TWP	252 ± 564	407 ± 656	365 ± 541	83 ± 70	51 ± 98	74 ± 115	71 ± 108	25 ± 34

^a‘Nan’ has been filled where there are no valid simulations.

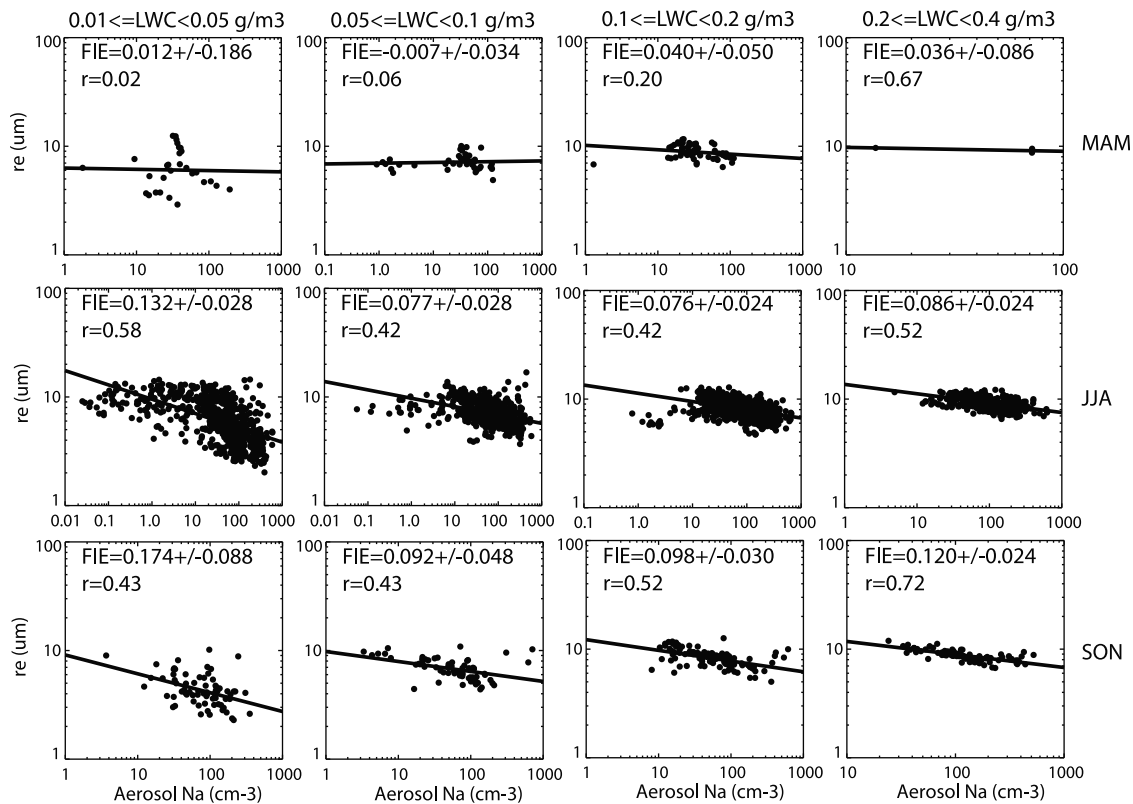


Figure 2. CAM5 simulated FIE for four ranges of LWC in spring (MAM), summer (JJA) and fall (SON) at NSA. The clouds considered here are non-precipitating low-level single layer liquid phase clouds from June 2008 to May 2010. Shown are scatterplots of cloud droplet effective radius (r_e) and the accumulation mode aerosol concentration (N_a). A log-log regression line is shown in each panel. The legend in each panel shows the FIE derived from the regression fit with 95% uncertainty estimates. Also indicated is the correlation coefficient between the logarithm of cloud r_e and N_a .

represented aerosol amounts with aerosol light scattering and considered all low-level single-layer liquid phase clouds just without ground precipitation. To see the impacts caused by different variables that represent aerosol amounts, we examined the FIE by using N_{CCN} at $S = 0.1\%$ (we do not have aerosol light scattering) to represent the aerosol amounts. The mechanism of the aerosol first indirect effect is that aerosols affect cloud N_d and r_e by acting as CCN. Therefore, we expect a generally better correlation between N_{CCN} and cloud r_e than between N_a and cloud r_e and a larger FIE by using N_{CCN} than using N_a . This is confirmed in Figure 3, which shows that FIE is about 0.10–0.25 for all three seasons by using N_{CCN} ($S = 0.1\%$) as a representation of aerosol loading. Particularly, the FIE in spring is highly sensitive to the variables that are used to represent aerosol amounts. To see the effects of precipitation, we examined the FIE by considering all low-level single-layer liquid phase clouds just with ground-level precipitation below 0.086 mm/day, for which it shows the FIE lies between 0.12 and 0.19 in summer and fall. These results imply that CAM5 has reasonably simulated the aerosol-cloud interaction at NSA, at least for summer and fall.

5.2. Variations of FIE With Geographical Location, Season, LWC and Aerosol Variable

[18] Figure 4 shows simulated FIE with 95% confidence intervals (outlines) to the linear-least squares regression slope between N_a and cloud r_e (left) and between N_{CCN} at

$S = 0.1\%$ and cloud r_e (right) for four ranges of LWC in different seasons at NSA, SGP and TWP. Only FIEs that are statistically significant are shown. Consistent with previous observational studies, the FIE simulated from CAM5 generally lies within a reasonable range with values below 0.33 and the FIE uncertainties are large at all three ARM sites.

[19] The sensitivity of FIE using N_a to ARM locations is examined. The FIE at SGP are mainly 0.12–0.16 in MAM, 0.17–0.22 in SON, and 0.10–0.13 (for LWC above 0.1 g m^{-3}) in DJF, with no statistically significant FIE in JJA and in DJF (for LWC below 0.1 g m^{-3}). These simulated FIE are consistent with the observed values (FIE between 0.02 and 0.17) from previous studies [Feingold *et al.*, 2003; Kim *et al.*, 2008] at SGP. At TWP, the FIE are mainly 0.08–0.23, 0.08–0.18, 0.06–0.12, 0.15–0.31 in MAM, JJA, SON, and DJF, respectively. In principle, there are generally no significant differences of simulated FIE for three ARM sites. Observational studies also show similar FIE values for SGP [Feingold *et al.*, 2003; Kim *et al.*, 2008] and NSA [Garrett *et al.*, 2004].

[20] Weak variations of FIE with seasons are found in Figure 4. The FIE is larger in DJF than other seasons at TWP. This seasonal variation is inversely related to the aerosol N_a and N_{CCN} at $S = 0.1\%$. As Table 1 shows, aerosol N_a and N_{CCN} (at $S = 0.1\%$) are much smaller in DJF than in other seasons, and they vary little for MAM, JJA and SON at TWP. The small aerosol amounts in DJF make the clouds at that period more susceptible to aerosols [Platnick and

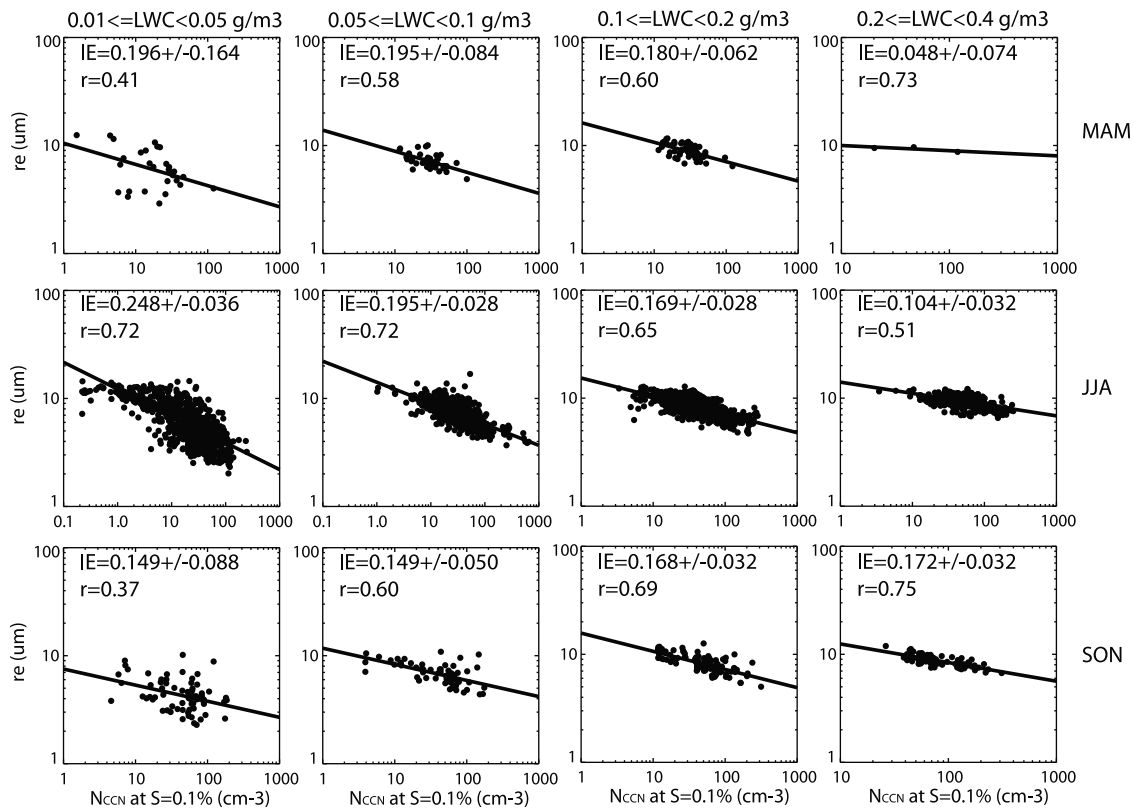


Figure 3. Same as Figure 1 except that the N_{CCN} at $S = 0.1\%$ is used to represent aerosol loading.

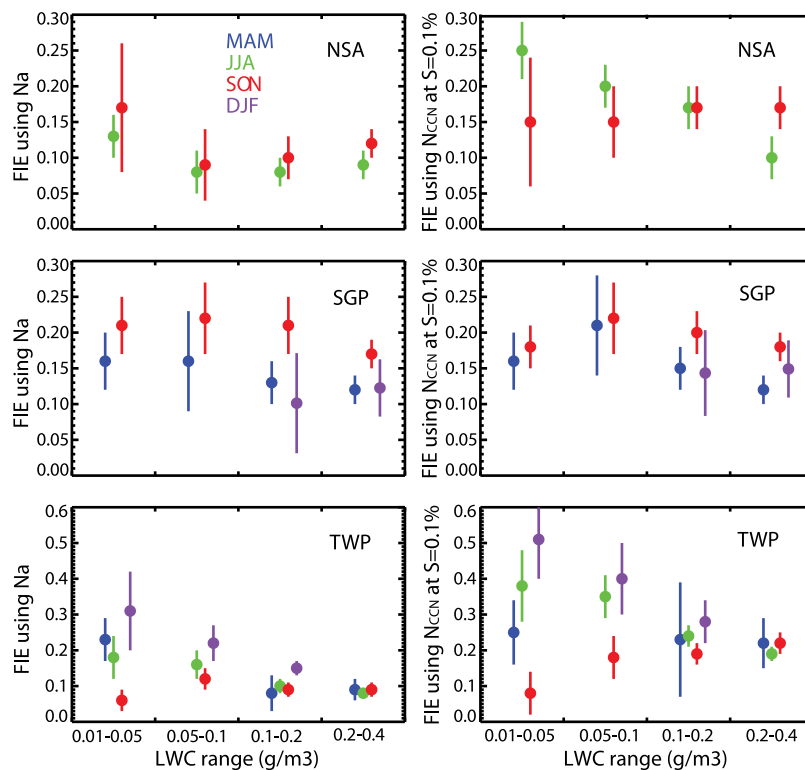


Figure 4. Simulated FIE with 95% confidence intervals (outlines) to the linear-least squares regression slope (left) between N_a and cloud r_c and (right) between N_{CCN} at $S = 0.1\%$ and cloud r_c for four ranges of LWC in different seasons (June 2008–May 2010) at NSA, SGP and TWP. Only FIEs that are statistically significant are shown.

Twomey, 1994]. Different from the TWP site, there are no significant seasonal variations of the FIE for NSA and SGP. Thus, there are no systematic strong seasonal variations for the FIE at three ARM sites. Quaas *et al.* [2009] have shown that there are also no systematic strong seasonal variations of the FIE for 14 individual regions based on satellite measurements.

[21] The FIE might vary with LWC. In general, cloud drop collision-coalescence may reduce cloud N_d just due to increasing liquid water, even in the absence of precipitation [McComiskey *et al.*, 2009]. Moreover, increasing LWC can reduce the competition of water vapor among cloud droplets and then increase droplet r_e . Therefore, an increase in LWC might reduce the FIE. However, if the aerosol loading that can serve as CCN is too heavy (like land area at SGP), this LWC effect on the FIE might be small. Figure 4 shows that the statistically significant FIE roughly decreases with LWC at TWP and NSA (except in SON), but has no clear sensitivity to LWC at SGP. A ground-based observational study [McComiskey *et al.*, 2009] has also found a reduction of FIE with increasing liquid amount for non-precipitating marine stratus clouds at Pt. Reyes, California.

[22] Figure 4 also shows that the FIE determined using N_{CCN} is generally larger than that calculated using N_a at all sites, particularly at coastal sites of NSA and TWP. While not shown, the correlation between cloud droplet r_e and N_{CCN} is generally better than that between cloud droplet r_e and N_a . Similarly, an observational study [McComiskey *et al.*, 2009] has also found the sensitivity of FIE on the choice of aerosol variable. Among the measures investigated by McComiskey *et al.* [2009], CCN is also the one for which the largest FIE is obtained. The sensitivity of FIE to the choice of aerosol variable indicates that consistent methods for the FIE quantification are required when we compare observations and model simulations.

6. Summary

[23] This study examines the aerosol first indirect effect simulated in CAM5 at three ARM sites. The FIE obtained from CAM5 forecast simulations is generally consistent with a large number of observational studies, suggesting that the two-moment cloud microphysics and its connection to aerosols recently implemented in CAM5 works reasonably well in the simulation of aerosol-cloud interactions for this type of low clouds. Wang *et al.* [2011] found that the aerosol total indirect effects from CAM5 is much larger than that from a multiscale modeling framework (MMF) model because of the too large response of LWP and precipitation to the aerosol change. If our study has general applicability for the FIE in other cloud types and locations, it suggests that efforts should be made to reduce other aerosol indirect effects such as cloud lifetime effect in CAM5. This may be a more difficult problem for GCMs with coarse resolutions.

[24] For non-precipitating low-level liquid clouds, the study also examines the sensitivity of simulated FIE to geographical location, season, cloud LWC, and choice of aerosol variable. In general, the FIE has no significant variations with location and has no systematic strong seasonal variations at examined ARM sites. Also, the FIE generally decreases with LWC at coastal NSA and TWP, but has no clear variation with LWC at SGP, which are possibly due to the decreasing cloud susceptibility with aerosol amounts.

Moreover, we found that the FIE is generally larger by using N_{CCN} rather than N_a as a proxy of aerosol amount. Similar sensitivities of the FIE to location, season, LWC and choice of aerosol variable have been found by observational studies.

[25] Finally, it is important to note that cloud r_e and N_d are influenced by interactions and feedbacks with aerosols, dynamics and thermodynamics. The effects of dynamics, thermodynamics, and aerosol chemical properties on the FIE are not discussed here, which will be a subject of our future studies.

[26] **Acknowledgments.** The study in LLNL is performed under the auspices of the U. S. Department of Energy, Office of Science, Office of Biological and Environmental Research by Lawrence Livermore National Laboratory under contract DE-AC52-07NA27344. The Pacific Northwest National Laboratory (PNNL) is operated for the DOE by Battelle Memorial Institute under contract DE-AC06-76RLO 1830. The efforts of the authors are supported by the Earth System Modeling program and Atmospheric Radiation Measurement Program of DOE's Climate and Earth System Division of the Office of Science.

[27] The Editor thanks Xiping Zeng and an anonymous reviewer for their assistance in evaluating this paper.

References

- Ackerman, A. S., O. B. Toon, D. E. Stevens, A. J. Heymsfield, V. Ramanathan, and E. J. Welton (2000), Reduction of tropical cloudiness by soot, *Science*, 288, 1042–1047, doi:10.1126/science.288.5468.1042.
- Albrecht, B. A. (1989), Aerosols, cloud microphysics and fractional cloudiness, *Science*, 245, 1227–1230, doi:10.1126/science.245.4923.1227.
- Bouya, Z., and G. P. Box (2011), Seasonal variation of aerosol size distributions in Darwin, Australia, *J. Atmos. Sol. Terr. Phys.*, 73(13), 2022–2033, doi:10.1016/j.jastp.2011.06.016.
- Costantino, L., and F.-M. Bréon (2010), Analysis of aerosol-cloud interaction from multi-sensor satellite observations, *Geophys. Res. Lett.*, 37, L11801, doi:10.1029/2009GL041828.
- Feingold, G., W. L. Eberhard, D. E. Veron, and M. Previdi (2003), First measurements of the Twomey indirect effect using ground-based remote sensors, *Geophys. Res. Lett.*, 30(6), 1287, doi:10.1029/2002GL016633.
- Garrett, T. J., C. Zhao, X. Dong, G. G. Mace, and P. V. Hobbs (2004), Effects of varying aerosol regimes on low-level Arctic stratus, *Geophys. Res. Lett.*, 31, L17105, doi:10.1029/2004GL019928.
- Grandey, B. S., and P. Stier (2010), A critical look at spatial scale choices in satellite-based aerosol indirect effect studies, *Atmos. Chem. Phys.*, 10, 11459–11470, doi:10.5194/acp-10-11459-2010.
- Han, Q., W. B. Rossow, and A. A. Lacis (1994), Near-global survey of effective droplet radii in liquid water cloud using ISCCP data, *J. Clim.*, 7, 465–497, doi:10.1175/1520-0442(1994)007<0465:NGSOED>2.0.CO;2.
- Harrison, L., J. Michalsky, and J. Berndt (1994), Automated multifilter rotating shadow-band radiometer: An instrument for optical depth and radiation measurements, *Appl. Opt.*, 33, 5118–5125, doi:10.1364/AO.33.005118.
- Kim, B.-G., S. E. Schwartz, M. A. Miller, and Q. Min (2003), Effective radius of cloud droplets by ground-based remote sensing: Relationship to aerosol, *J. Geophys. Res.*, 108(D23), 4740, doi:10.1029/2003JD003721.
- Kim, B.-G., M. A. Miller, S. E. Schwartz, Y. Liu, and Q. Min (2008), The role of adiabaticity in the aerosol first indirect effect, *J. Geophys. Res.*, 113, D05210, doi:10.1029/2007JD008961.
- Liu, X., *et al.* (2011), Toward a minimal representation of aerosol direct and indirect effects: Model description and evaluation, *Geosci. Model Dev. Discuss.*, 4, 3485–3598, doi:10.5194/gmdd-4-3485-2011.
- McComiskey, A., and G. Feingold (2008), Quantifying error in the radiative forcing of the first aerosol indirect effect, *Geophys. Res. Lett.*, 35, L02810, doi:10.1029/2007GL032667.
- McComiskey, A., and G. Feingold (2012), The scale problem in quantifying aerosol indirect effects, *Atmos. Chem. Phys.*, 12, 1031–1049, doi:10.5194/acp-12-1031-2012.
- McComiskey, A., *et al.* (2009), An assessment of aerosol-cloud interactions in marine stratus clouds based on surface remote sensing, *J. Geophys. Res.*, 114, D09203, doi:10.1029/2008JD011006.
- Morrison, H., and A. Gettelman (2008), A new two-moment bulk stratiform cloud microphysics scheme in the community atmosphere model, version 3 (CAM3), part I: Description and numerical tests, *J. Clim.*, 21, 3642–3659, doi:10.1175/2008JCLI2105.1.

- Neale, R., et al. (2010), Description of the NCAR Community Atmosphere Model (CAM 5.0), *Tech. Note NCAR/TN-486+STR*, Natl. Cent. for Atmos. Res., Boulder, Colo. [Available at http://www.cesm.ucar.edu/models/cesm1.0/cam/docs/description/cam5_desc.pdf.]
- Pandithurai, G., T. Takamura, J. Yamaguchi, K. Miyagi, T. Takano, Y. Ishizaka, S. Dipu, and A. Shimizu (2009), Aerosol effect on cloud droplet size as monitored from surface-based remote sensing over East China Sea region, *Geophys. Res. Lett.*, *36*, L13805, doi:10.1029/2009GL038451.
- Phillips, T. J., et al. (2004), Evaluating parameterizations in GCMs: Climate simulation meets weather prediction, *Bull. Am. Meteorol. Soc.*, *85*, 1903–1915, doi:10.1175/BAMS-85-12-1903.
- Platnick, S., and S. Twomey (1994), Remote sensing the susceptibility of cloud albedo to changes in drop concentration, *Atmos. Res.*, *34*, 85–98, doi:10.1016/0169-8095(94)90082-5.
- Quaas, J., et al. (2009), Aerosol indirect effects—General circulation model intercomparison and evaluation with satellite data, *Atmos. Chem. Phys.*, *9*, 8697–8717, doi:10.5194/acp-9-8697-2009.
- Rosenfeld, D., and G. Feingold (2003), Explanation of discrepancies among satellite observation of aerosol indirect effects, *Geophys. Res. Lett.*, *30*(14), 1776, doi:10.1029/2003GL017684.
- Shao, H., and G. Liu (2006), Influence of mixing on evaluation of the aerosol first indirect effect, *Geophys. Res. Lett.*, *33*, L14809, doi:10.1029/2006GL026021.
- Tang, J. P., P. C. Wang, M. Z. Duan, H. B. Chen, X. A. Xia, and H. Liao (2011), An evidence of aerosol indirect effect on stratus clouds from the integrated ground-based measurements at the ARM Shouxian site, *Atmos. Oceanic Sci. Lett.*, *4*(2), 65–69.
- Twomey, S. (1977), The influence of pollution on the shortwave albedo of clouds, *J. Atmos. Sci.*, *34*, 1149–1152, doi:10.1175/1520-0469(1977)034<1149:TIOPOT>2.0.CO;2.
- Wang, M., S. Ghan, M. Ovchinnikov, X. Liu, R. Easter, E. Kassianov, Y. Qian, and H. Morrison (2011), Aerosol indirect effects in a multi-scale aerosol-climate model PNNL-MMF, *Atmos. Chem. Phys. Discuss.*, *11*, 3399–3459, doi:10.5194/acpd-11-3399-2011.
-
- J. S. Boyle, S. A. Klein, S. Xie, Y. Zhang, and C. Zhao, Atmosphere, Earth, and Energy Division, Lawrence Livermore National Laboratory, 7000 East Ave., Mail Code L-103, Livermore, CA 94550, USA. (zhao6@llnl.gov)
- X. Liu, Pacific Northwest National Laboratory, Richland, WA 99352, USA.